EWOD driven cleaning of bioparticles on hydrophobic and superhydrophobic surfaces

M. Jönsson-Niedziółka,†*[ad] F. Lapierre,†[a] Y. Coffinier,[ab] S. J. Parry,[c] F. Zoueshtiagh,[a] T. Foat,[c] V. Thomy[a] and R. Boukherroub[ab]

Received 15th July 2010, Accepted 13th October 2010
DOI: 10.1039/c0lc00203h

Environmental air monitoring is of great interest due to the large number of people concerned and exposed to different possible risks. From the most common particles in our environment (*e.g.* by-products of combustion or pollens) to more specific and dangerous agents (*e.g.* pathogenic micro-organisms), there are a large range of particles that need to be controlled. In this article we propose an original study on the collection of electrostatically deposited particles using electrowetting droplet displacement. A variety of particles were studied, from synthetic particles (*e.g.* Polystyrene Latex (PSL) microsphere) to different classes of biological particle (proteins, bacterial spores and a viral simulant). Furthermore, we have compared ElectroWetting-On-Dielectric (EWOD) collecting efficiency using either a hydrophobic or a superhydrophobic counter electrode. We observe different cleaning efficiencies, depending on the hydrophobicity of the substrate (varying from 45% to 99%). Superhydrophobic surfaces show the best cleaning efficiency with water droplets for all investigated particles (MS2 bacteriophage, BG (*Bacillus atrophaeus*) spores, OA (ovalbumin) proteins, and PSL).

1. Introduction

Air pollution is one of the most challenging problems where early pollutant detection can help in reducing exposure risks to the population. The pollution can come from some of the most common particles in our environment (*e.g.* by-products of combustion or pollens) to more dangerous agents (*e.g.* pathogenic micro-organisms). Aerosol collection systems that are currently available, typically present several drawbacks such as their moderate concentration ratios, high power requirement and difficulty in integration of the collection stage with the identification stage. Lab on chip systems have proved their potential in a large number of applications such as cell based assays, biochemical operations, *in situ* detection or analysis and environmental control.[1–5] A lab on chip based system for collection and analysis of airborne microparticles would be useful for cost effective monitoring of air quality, especially in environments where pure water is a scarce resource. Proof of concept devices have usually been limited to microparticle collection in a more or less complex microfluidic system. Particle collection by filtration or electrostatic techniques has already been reported in the literature. To our knowledge the first report on the integration of a collecting device with a microfluidic system was made by Fair *et al.*[6] Once the airborne particles were deposited on a planar electrode by impacting them with the surface, a droplet of solvent was moved across the chip in order to collect and to concentrate the particles inside the small amount of liquid. Their set up required heavy, very specific equipment for the deposition. Moreover, the samples used were molecular species in aerosol particles and were collected by dissolving them in a droplet of suitable solvent.

Desai *et al.*[7] have shown that electrostatic collection (based on a dielectrophoretic transportation system) of sub micrometre particles gave a remarkable efficiency, of about 90%. But in order to electrostatically transport 5–10 μm size particles successfully the authors needed to use very specific combinations of insulation thickness, electrode geometry and insulation material.

Zhao and Cho proposed an interesting sweeping system made of a filtering membrane inside which EWOD driving electrodes were positioned.[8,9] However, their microsystem needed a complex and expensive production process. Furthermore, the authors presented results with particles sampling from flat solid surfaces (coated by a hydrophobic Teflon layer) and only mention the possibility of using holes as a filtration system inside the electrowetting structure. The particles that were tested were glass and PTFE beads with different coatings (from superhydrophilic to superhydrophobic), with a diameter between 2 and 8 μm. The sampling efficiency ranged between 68%, for PTFE, and 93% for glass beads. No experiments were carried out using real biological particles, the shape and coating of which differ from synthetic ones.

Tan *et al.*[10] proposed a microparticle collection and concentrating device using Surface Acoustic Waves (SAW). They have shown that results obtained with synthetic microparticles (in their case, polystyrene and melamine, with a 16–55% collecting efficiency) are not a substitute for the study of biological micro organisms (45–68% for pollens and 61–70% for *Escherichia coli* bacteria).

[a]*IEMN, Université Lille Nord de France, Avenue Poincaré, Lille, France. E-mail: vincent.thomy@iemn.univ-lille1.fr; Fax: +33 (0)3 20 19 78 80; Tel: +33 (0)3 20 19 79 51*
[b]*IRI, Université Lille Nord de France, Haute Borne, Lille, France. E-mail: rabah.boukherroub@iri.univ-lille1.fr; Fax: +33 (0)3.62.53.17.01; Tel: +33 (0)3.62.53.17.24*
[c]*DSTL, Porton Down, Salisbury, Wiltshire, SP4 0JQ, United Kingdom. E-mail: tgfoat@dstl.gov.uk; Tel: +44 (0)1980 614623*
[d]*Institute of Physical Chemistry, Polish Academy of Sciences, ul. Kasprzaka 44/52, 01-224 Warsaw, Poland. E-mail: martinj@ichf.edu.pl*
† Authors contributed equally to the article and share first co-authorship.

Recently Bushan *et al.*[11] investigated the interaction between droplet impact, representing artificial rain, and SiC particles in the size ranges of 1–10 μm and 10–15 μm previously deposited on flat hydrophilic and hydrophobic, and nano, micro and hierarchically structured superhydrophobic surfaces. They showed that self-cleaning performances were obtained with surfaces with geometrical scale effects that lowered adhesion and hysteresis.

From these earlier experiments it is clear that several points need to be investigated in order to enhance the collecting efficiency of an integrated system; the deposition system has to be as simple as possible to be integrated with the microfluidic part and the particles studied have to cover a wide range of relevant microorganisms or bioparticles.

In this paper we propose an original study differing from the cited articles by the use of several different particles as well as tests with alternative cleaning agents where pure water is not sufficient. The particles include the standard model system, synthetic polystyrene spheres (PSL), as well as several bioparticles with different sizes and wettability properties as presented in Table 1.

Furthermore, in the present study the influences of different EWOD and fluidic system parameters on the collecting efficiency were investigated. In particular, we probed the influence of the electrowetting applied voltage, the number of back and forth movements of the droplet and its velocity driven by EWOD. We also investigated the influence of the counter electrode surface by using both hydrophobic and superhydrophobic coatings.

2. Reagents and materials

2.1. Electrowetting on dielectric (EWOD)

Electrowetting on dielectric (EWOD) microdevices have already been demonstrated to allow basic microdroplet manipulations on totally hydrophobic surfaces such as creating, cutting, merging and transporting.[12,13] Usually EWOD results are obtained with a set up consisting of two hydrophobic parallel plates between which microdroplets of liquid are sandwiched. Our group has previously demonstrated that the utilization of nanotextured silicon nanowire surfaces for one of the two plates, has allowed matrix-free mass-spectrometry analysis (DIOS analysis).[14] Furthermore, we can speculate that the insertion of a superhydropobic surfaces as the EWOD counter electrodes can reduce the flow resistance and provides the advantage of artificially reproducing some of the self-cleaning properties of the famous Lotus leaf.[15–18] In this article, we investigate both hydrophobic and superhydrophobic surfaces as counter electrodes in a conceptual device for the collection of bioparticles from the electrode surface using an EWOD actuated droplet.

In brief, droplet motion by electrowetting relies on the local modification of the shape (contact angle) of the drop lying on a hydrophobic surface through an applied voltage.[19] With an electrode network, it is then possible to move a droplet from one electrode to another as seen in Fig. 1. The base (upper part) contains the EWOD electrodes covered by an insulating layer and a hydrophobic material. An additional dielectric layer covering the base electrodes is necessary to avoid electrolysis of the (water) droplet. The (super)hydrophobic cover (lower part) which is conductive is connected to the ground and plays the role of the counter electrode.[20]

2.2. Device fabrication; the base plate

The electrodes are made on 75 mm diameter glass substrates by deposition of a 20 nm nickel layer by cathodic sputtering (Fig. 2 a.1). This thin metal layer is used to create a transparent network of electrodes which are patterned by photolithography (Fig. 2 a.2–3) and developed through wet etching (H_2O/HNO_3, 1 : 3 v/v, 1min). The photoresist is then removed in successive baths of acetone and isopropyl alcohol, rinsed with deionised water and dried under a stream of nitrogen (Fig. 2 a.4). Then, the dielectric layer (Su-8 2002, $\varepsilon_r = 3.2$ at 10 MHz) is deposited by spin-coating (Fig. 2 a.5). This is to obtain a thin, transparent insulating layer on the conductive electrode. The choice of the photosensitive Su-8 as an insulator is based on the excellent dielectric properties of the material which allows the creation of a layer thin enough for proper EWOD function while still preventing electric breakdown at the very high fields applied during EWOD operation (≥200 V μm^{-1}).[21] Finally, a thin hydrophobic layer (Cytop® CTL-809M) is spin-coated to complete the system (Fig. 2 a.6). Contact angle (CA) and contact angle hysteresis (CAH) are approximately 112° and 11°, respectively. A picture of the final system is shown

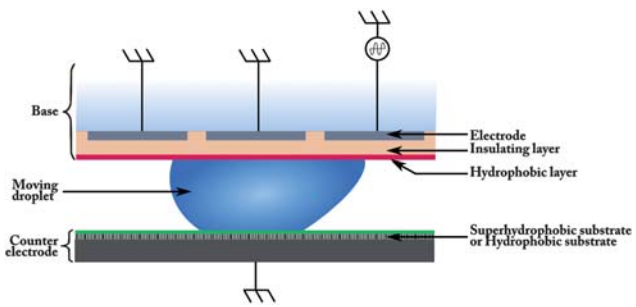

Fig. 1 Set up of the EWOD platform. The counter electrode surface is either hydrophobic or superhydrophobic. The base is composed of Ni (electrodes), Su-8 (dielectric layer, e = 2μm) and Cytop® (hydrophobic coating).

Table 1 Particle characteristics

Particles	Size, form	Wettability properties	Aggregation
OA (Ovalbumin)	6.4 nm, globular form	Hydrophobic	Yes
BG (*Bacillus atrophaeus*)	0.8 × 1–1.5 μm, elliptic form	Lower hydrophobicity, dependent of pH	Yes, formation of 1–9 μm aggregates
MS2 (Bacteriophage)	28 nm, symmetric icosahedral	Relatively hydrophobic	Yes, interaction with protein capsids
PSL (Polystryrene beads)	1 μm, spherical	Hydrophobic	No

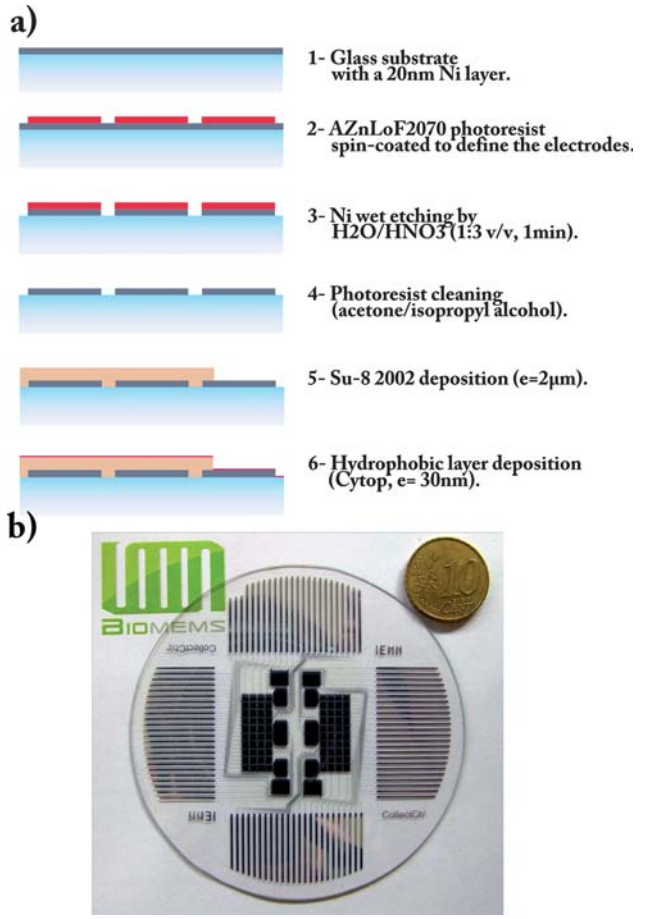

Fig. 2 (a) Description of the fabrication of the base by lithography. (b) Picture of the base: the 96 electrodes are individually adressable.

Fig. 2b integrating 96 individually addressable electrodes on a 3″ glass wafer.

2.3. Device fabrication; the counter electrode

Hydrophobic and superhydrophobic surfaces have been produced in order to test two types of counter electrode according to their particle collection efficiency.

2.3.1. Hydrophobic surface. The hydrophobic surface was produced with the same hydrophobic material as the base. After different cleaning steps on highly doped silicon wafer (acetone/isopropyl alcohol and piranha bath (H_2SO_4/30% H_2O_2 1 : 1 v/v) for 15 min at 80 °C), Cytop® is deposited by spin coating. CA and CAH were the same as on the base.

2.3.2. Superhydrophobic surface. The superhydrophobic surfaces were synthesized on single-side polished silicon (100) oriented n-type wafers (*Siltronix*, *France*) (phosphorus-doped, 0.009–0.01 Ω cm^{-1} resistivity). First, the substrate was cleaned in a piranha bath, and rinsed with deionized water for 10 min in an ultrasonic bath. Then, the substrate was directly immersed in a HF (5.25 M)/$AgNO_3$ (0.04 M) (1 : 1 v/v) aqueous solution for 10 min at 54 °C, leading to a wet etching of the silicon wafer. Then the substrate was rinsed by deionized water and dried by a nitrogen flow. As seen in Fig. 3a, the silicon nanostructures are covered by silver dendrites. To remove the silver, the substrate was immersed for 8 h in H_2O/HCl/HNO_3 (1 : 1 : 1 v/v/v) at room temperature, rinsed with deionized water and dried under a nitrogen flow. The nanostructures' dimensions were in the range of hundreds of nanometres width, and were 1 µm height, as seen in the cross-sectional SEM view (Fig. 3b–c). A chemical modification of the surface with a conformal octadecyltrichlorosilane (OTS) layer led to the formation of a superhydrophobic surface with a contact angle of 160° with low hysteresis (0–2°). The surface roughness combined with the low surface energy induced by the surface modification ensured air trapping between the substrate and the liquid droplets, which is necessary to achieve superhydrophobicity.[22,23]

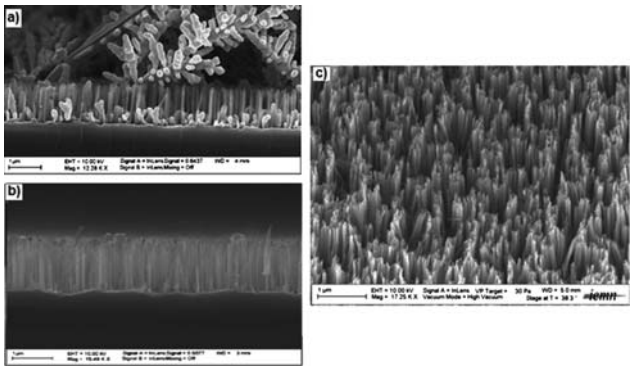

Fig. 3 Cross-section SEM images of the silicon nanostructures substrate (a) before and (b) after H_2O/HCl/HNO_3 rinsing step. (c) Tilted SEM image of the nanostructures.

2.4. Droplet actuation

Droplet displacements by EWOD were carried out as follows: A square-wave electrical signal is obtained through a signal generator (CENTRAD GF 265, ELC, France) with a 0.5 to 21 V_{PP} output at 1 kHz, coupled to a 50 dBm high-voltage amplifier (TEGAM, USA). The resulting voltage can be varied from 12.5 V_{TRMS} ($V_{TRMS} = V_{PP}/2$) to 250 V_{TRMS}. The signal is fed into a home-built 24-way electric relay card so that the voltage on the electrodes can be controlled individually through a LabView program. The switching time between two electrodes can be adjusted from 3 ms to 1 s to control the droplet velocity. The counter electrode is placed onto a Teflon holder. The distance (or gap) between the electrode and the counter electrode is fixed by conductive spacers. Experiments have been realized with a 300 µm spacer height which is calibrated for a 1 µl droplet displacement according to the EWOD electrode dimensions ($2 \times 2\ mm^2$). A high speed camera (Photron; 20 000 frames/s, with a resolution of 512 × 128 pixels) was used for recording the droplet displacement. The simplicity of our system allowed portable, automatic, and high speed manipulations. The droplet actuation was performed with different applied voltages ranging from 60 to 110 V_{TRMS} and with different actuation time on each electrode.

2.5. Particle deposition using electrostatic precipitation

Fig. 4 shows the setup for the electrostatic precipitation experiments. Aerosol was generated using a mini-nebuliser containing

either a water suspension or solution of the micro-organisms, PSL or protein; the nebulisation process imparts a small negative or positive charge to the aerosol droplets. The charged aerosol was passed into a conditioning chamber to allow time for the water to evaporate leaving just the dry particles. An electric potential of −1000 V was applied to the EWOD counter electrode surface and the aerosol was drawn through the electrostatic precipitator using the integral pump in the Grimm aerosol spectrometer 1.109, connected downstream. A proportion of the positively charged aerosol was then precipitated onto the EWOD surface. The remaining aerosol passed through the precipitator and the size distribution was measured using the aerosol spectrometer. The whole system was run with various concentrations of suspension or solution, aerosol generation times and precipitation sample times to achieve the desired deposit concentration on the EWOD surface.

3. Experiments

The droplet displacement was carried out on an array of electrodes. Typically the droplet was moved back and forth along five electrodes. The number of passes was varied from one single pass in one direction up to, in some experiments, as many as 500 passes back and forth. The voltage applied to the electrode to actuate the droplet movement was a square signal with a frequency of 1kHz. The applied voltage was typically kept at 60 V_{TRMS}. However, in the case of high concentration of particles, degradation of the electrode base Cytop® -coating during the measurements or the presence of dust-particles and other imperfections, the voltage had to be increased occasionally up to 120 V_{TRMS}.

Experiments were performed with four types of particles (*cf.* Table 1) using different deposition times leading to concentrations ranging from about 10 000 particles mm^{-2} to 250 000 particles mm^{-2}. The surfaces with the deposited particles were placed as counter-electrodes. The connection with ground was made by placing the samples on an electrically conducting base. A 1μl deionised water droplet was then deposited on the electrode using a micro-pipette and the base electrode was put in place on top of the counter-electrode. In the case where surface cleaning with water was inefficient, experiments were conducted using aqueous solutions of Tween 20 instead of deionised water, to see if the inclusion of a surfactant would increase the efficiency. On hydrophobic Cytop® surfaces a solution of 0.01% Tween 20 in water could be used for displacement, whereas more concentrated solutions were too viscous and prevented droplet movement. On superhydrophobic surfaces the addition of surfactant to the droplet increased the surface wetting and caused the droplet to be impaled into the nanostructure. During the experiments the droplet was moved back and forth a number of times along a line. Afterwards, the electrode plate would be lifted, the droplet removed and the counter-electrode taken off the setup and placed under microscope for observation (Fig. 5).

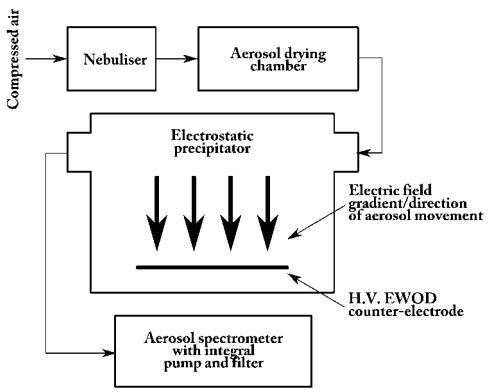

Fig. 4 Setup for the electrostatic precipitation experiments.

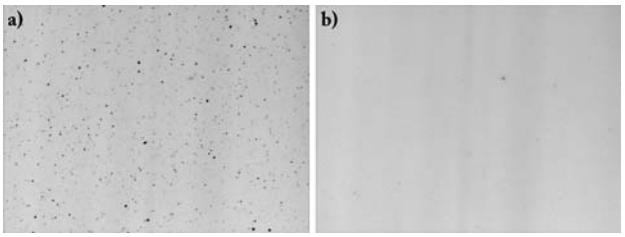

Fig. 5 Optical micrographs of the particles on the hydrophobic cover electrode (a) before and (b) after the passage of the droplet.

The particle counting was performed using an automated image analysis (*ImageJ*) of microscope images. In the case of nanostructured surfaces the images were recorded using fluorescent microscopy. High resolution pictures were taken outside (~5 pictures) and inside (~15 pictures) the droplet pathway to get an accurate measure of the amount of particles before and after EWOD cleaning. Each image is analysed through an *ImageJ* routine and gives the number of particle per unit area. We define the cleaning efficiency with eqn (1):

$$\%_{\text{cleaningefficiency}} = \left(1 - \frac{N_{in}}{N_{out}}\right) * 100 \quad (1)$$

where N_{in} is the average number of particles inside the droplet pathway and N_{out} is the average number of particles outside the droplet pathway.

4. Results and discussion

4.1. Droplet movement characterisation

The average droplet velocity was characterised using the high speed camera and calculated with $S_D = l/t$, with l, the length of an electrode ($l = 2$ mm), and t the time for the advancing shape of the droplet, starting from the end of the first electrode, to reach the end of the second one. Fig. 6 represents 6 different shapes (top and side views) of the droplet at different times during the displacement on a superhydrophobic surface.

On the side view, the contact angle has been measured: (1) the first electrode is actuated; the droplet spreads out on it. Left and right contact angle (LCA and RCA) are around 80° ± 5°. (2) When the second electrode is on, LCA increases to 100° ± 5°; this side of the droplet is not actuated. On the contrary, RCA decreases to 65°; the droplet starts to move toward the second electrode. (3)-(4)-(5) RCA varies between 50°–60° and LCA decreases from 100° to 70°; the trailing edge of the droplet is pulled by its leading edge. (6) The droplet reaches the second electrode, still actuated; LCA and RCA are around 80°. The CA of the droplet on the counter electrode (bottom part of the

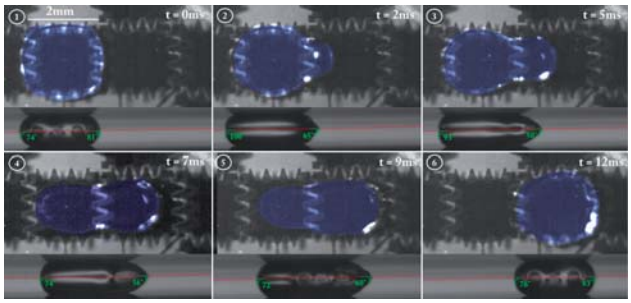

Fig. 6 Pictures of the droplet displacement on superhydrophobic surface (top and side views). Voltage applied: 62.5 V_{TRMS}. The droplet has been artificially coloured to improve clarity. Each electrode was 2 mm^2.

pictures), stays around 160° whichever electrode is actuated. A more detailed microfluidic study of the contact angle and shear stress during EWOD droplet displacement is beyond the scope of this paper and is the topic of a manuscript in preparation.

Meanwhile, Fig. 7 shows the relationship between the Labview switching time and the droplet average velocity. The average droplet speed was approximately 130 mm s^{-1} or 90 mm s^{-1} for a superhydrophobic or hydrophobic surface, respectively, even if the switching time between two electrodes was increased. However, it was observed that for a switching time close to the critical values (13 ms and 20 ms for superhydrophobic and hydrophobic surfaces, respectively), the droplet motion could reach 166 mm s^{-1} or 121 mm s^{-1} depending of the hydrophobicity of the counter electrode. This may have been due to the inertia of the droplet during the displacement which would have pushed it to the next electrode. At these critical values, the droplet motion is continuous; the droplet has no time to come to rest at the electrode before moving on. For switching times which were shorter than the critical values the droplet did not move to the next electrode. In conclusion, superhydrophobic counter electrode surfaces increase the average droplet speed with about 30% compared to hydrophobic ones.

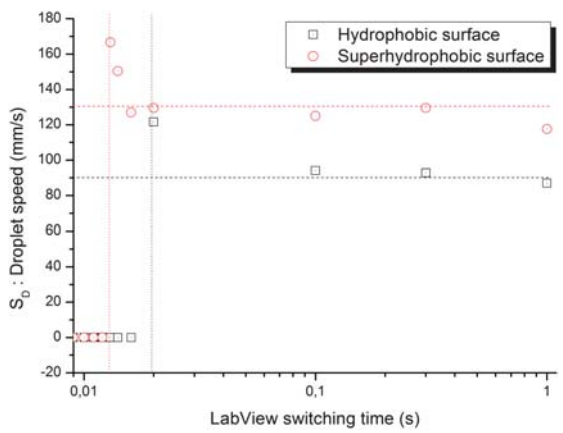

Fig. 7 Average droplet speed between two electrodes during the EWOD displacement *versus* the switching time. Dashed lines represent the mean of the droplet speed for the two super- (red) and hydrophobic (black) surfaces. Dotted lines represent the critical switching time when the droplet reaches its maximum speed.

To the best of our knowledge this is the first comparison of this parameter inside a EWOD droplet based microsystem using a hydrophobic or a superhydrophobic cover.

4.2. Surface cleaning

Fig. 8 show the cleaning efficiency on super- (black) and hydrophobic (red) surfaces for different particles. The reported error bars correspond to one standard deviation of the particle numbers in the recorded images.

The experiments performed with PSL particles confirm the results of Zhao *et al.* who successfully demonstrated the cleaning efficiency by electrowetting-actuated droplets of particles (glass beads and polystyrene beads, from 2 to 8 μm diameter) with different degree of wettability.[8,9] They showed that the sampling efficiency was over 93%, and in particular 98% for the biggest (7.9 μm) hydrophilic glass beads. Our experiments with 1 μm polystyrene particles show a cleaning efficiency of more than 90% after just one pass (see Table 2). This result was obtained regardless of whether the surface was hydrophobic or superhydrophobic. Furthermore, increasing the number of passes did not improve the cleaning efficiency.

For the BG spore, the analysis showed a significant decrease in cleaning efficiency on the Cytop® surfaces compared to the superhydrophobic surfaces. On the nanostructured superhydrophobic surfaces, the cleaning efficiency was close to 100% whereas on the hydrophobic surfaces more than half of the deposited particles remained on the surface after cleaning. The statistical analysis showed that on Cytop® samples there was a significant effect of particle concentration, where the surface with more BG is more efficiently cleaned, though still far less than on superhydrophobic surfaces. Using 0.01% Tween instead of deionised water as a liquid droplet produced similar results.

Experiments carried out with the protein OA underscores the importance of the particles' properties on the resulting cleaning efficiency. Indeed, except for in very low surface concentrations, the protein inhibits the movement of the droplet. The analysis shows that the difference in cleaning efficiency between hydrophobic and superhydrophobic surfaces is not statistically significant. This is mostly due to a low number of successful

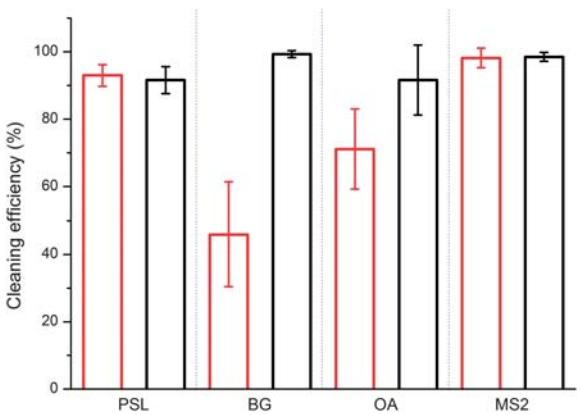

Fig. 8 Different particles collect efficiency (synthetic polystyrene microparticles (PSL), spores (BG), proteins (OA), bacteriophage (MS2)) on hydrophobic (red) and superhydrophobic (black) surfaces using deionised water.

Table 2 Summary of the particle collection efficiency

	Hydrophobic surfaces	Superhydrophobic surfaces
PSL	93 ± 3.2%	92 ± 4.0%
BG	46 ± 16%	99 ± 1.3%
OA	71 ± 12%	92 ± 11%
MS2	99 ± 1.3%	98 ± 2.9%

droplet displacements. To illustrate the difficulty encountered with OA, even at the highest voltage only at around 10% of the tries actuation was possible, and even then usually only for a single pass. However, in the few cases where the droplet actually moved, the cleaning was quite efficient, creating a positive statistical bias. This result is in agreement with observations by Koc *et al.*[24] on nano-scale superhydrophobic substrates. They show that proteins readily adsorb on superhydrophobic surfaces, but also are quite efficiently removed by water flow. The variance in the cleaning efficiency was higher with OA than any other tested sample. On the superhydrophobic surfaces the efficiency was 92 ± 11% and on the Cytop® surfaces 71 ± 12%. Furthermore, the OA covered surface was the only superhydrophobic surface where droplet actuation with Tween was possible. It seems clear that the OA prevents the Tween from penetrating into the pores of the superhydrophobic surface. However, the details of protein interaction with superhydrophobic surfaces are still largely unknown.[24] The cleaning efficiency with Tween was the same as that of water.

The surface with the viral simulant MS2 shows no difference in cleaning efficiency on the different surfaces. As with the polystyrene, most of the deposited particles (>95%) are removed in every experiment.

Interestingly, there seems to be no effect of the number of passes by the droplet on the amount of particles it removed from the surface. This means that most of the particles that can be removed are done so on the first pass of the drop. This is a very useful result for future applications, as it reduces both the amount of time needed to remove particles from a surface and the possible fouling of the EWOD base by particle redeposition.

Redeposition of particles on the base electrodes can prevent the droplet from moving. Only at very high particle concentrations, especially using proteins, together with a large number of droplet passes was EWOD base fouling problematic. Thus, the issue of redeposition is in most cases a preventable problem.

No difference in the cleaning efficiency as a function of actuation voltage was detected.

As a comparison to the EWOD displacement some experiments were also performed where the droplet was moved across the surface manually. In those experiments, the cleaning efficiency on Cytop® was comparable to the EWOD cleaning for all bioparticles. For BG, the cleaning efficiency was 64 ± 9% and for OA 72 ± 10%. In the case of superhydrophobic surfaces the cleaning efficiency was significantly higher for the EWOD actuated droplets. The exception was for MS2 which is totally cleaned off using both actuation methods. One reason for the higher efficiency with superhydrophobic surfaces is possibly because of the actuation frequency (1 kHz) of the droplet during the EWOD displacement. As already depicted by other groups,[25–27] AC voltage induce local oscillations of the droplet near the contact line of the base. These observations have been made using a classical needle or a 1D EWOD setup. In all cases, the droplet was not covered by a counter electrode, vibrations being only attenuated by the base. In our setup, as observed by high-speed camera, the utilization of a hydrophobic counter electrode for EWOD displacements led to a high vibration attenuation. On the contrary, the use of a superhydrophobic cover does not limit the propagation of these oscillations. This negligible effect of the nanotextured surface on the droplet movement, compared to the hydrophobic one, is also pointed out by the difference of the average droplet speed detailed in Fig. 7. Although a detailed description of these aspects is beyond the scope of this manuscript, we can assume that the droplet oscillation, induced by AC EWOD, improves the particle sweeping. This point explains the similar results between manual cleaning and EWOD cleaning on hydrophobic surfaces.

5. Conclusions

We have performed measurements on the cleaning efficiency of EWOD actuated droplets on hydrophobic as well as superhydrophobic surfaces. The measurements were performed using several different bioparticles. Especially on hydrophobic surfaces (Si coated by Cytop®), we have shown that the cleaning efficiency depends strongly on the nature of the deposited particles. PSL and MS2 viral simulant are almost completely removed (90%) from the hydrophobic surface with only one pass whereas BG and OA particles are more difficult to recover (45% to 70% clean), even with the use of a surfactant.

In the case of superhydrophobic, nanostructured surfaces we showed that they, due to their intrinsic self-cleaning behaviour popularly known as the "Lotus effect", are efficiently cleaned of all tested particles. Even though the use of surfactants is a problem with such a surface (*i.e.* Tween 20 is a wetting agent and when a droplet containing Tween 20 is placed on a superhydrophobic surface it wets the surface and cannot be actuated), the use of water allows nearly complete cleaning of the surface. However, also in the case of these surfaces the particle properties are of importance. As was shown in the case of the protein OA, the particles may change the surface properties making droplet displacement impossible.

Our results show a concept EWOD system for efficient cleaning of a surface that could easily be integrated with a deposition and/or analysis system. With an adjustable distance between the base and the cover, the same electrodes could be used for both electrostatic precipitation and EWOD droplet actuation. With the inclusion of pre-charging of the areosol before deposition as well as by adjusting the depostion potential and flowrate the system could be optimised for highly efficient aerosol collection.[28,29] Particles deposited on a surface can be collected in a droplet and moved to an analysis station. We also showed that the collection is efficient and that a single pass of the droplet is enough to collect more than 90% of the deposited particles from a superhydrophobic surface. However, the experiments also show that the wetting properties of the particles can have a significant influence on the collection efficiency, in particular with proteins, well known for their sticking ability. These results underscore the importance of testing EWOD systems using real biological particles instead of idealised model systems like polystyrene or glass beads.

Acknowledgements

© Crown copyright. Published with the permission of the Defence Science and Technology Laboratory on behalf of the Controller of HMSO. The authors thank Maxime Harnois at the Microfluidics Lab (IEMN-UMR8520) for technical support in developing the EWOD mask and Christine Faille for her kind support for microfluidic experiments with biological particles at Institut National de la Recherche Agronomique (INRA, UR638 PIHM). MJN gratefully acknowledges financial support from PAN-CNRS project # 22516.

References

1 M. Abdelgawad, M. W. L. Watson and A. R. Wheeler, *Lab Chip*, 2009, **9**, 1046–1051.
2 D. Mark, S. Haeberle, G. Roth, F. v. Stetten and R. Zengerle, *Chem. Soc. Rev.*, 2010, **39**, 1153–1182.
3 R. Gorkin, J. Park, J. Siegrist, M. Amasia, B. S. Lee, J.-M. Park, J. Kim, H. Kim, M. Madou and Y.-K. Cho, *Lab Chip*, 2010, **10**, 1758–1773.
4 J. Lee, S. A. Soper and K. K. Murray, *Anal. Chim. Acta*, 2009, **649**, 180–190.
5 G. M. Whitesides, *Nature*, 2006, **442**, 368–373.
6 R. B. Fair, A. Khlystov, V. Srinivasan, V. K. Pamula and K. N. Weaver, *Proc. SPIE*, Philadelphia, PA, USA, 2004, pp. 113–124.
7 A. Desai, S.-W. Lee and Y.-C. Tai, *Sens. Actuators, A*, 1999, **73**, 37–44.
8 Y. Zhao and S. K. Cho, *Lab Chip*, 2006, **6**, 137–144.
9 Y. Zhao, S. K. Chung, U.-C. Yi and S. K. Cho, *J. Micromech. Microeng.*, 2008, **18**, 025030.
10 M. K. Tan, J. R. Friend and L. Y. Yeo, *Lab Chip*, 2007, **7**, 618–625.
11 B. Bhushan, Y. C. Jung and K. Koch, *Langmuir*, 2009, **25**, 3240–3248.
12 S. K. Cho, H. Moon and C.-J. Kim, *J. Microelectromech. Syst.*, 2003, **12**, 70–80.
13 S. K. Cho and H. Moon, *Biochip. J.*, 2008, **2**, 79–96.
14 N. Verplanck, Y. Coffinier, V. Thomy and R. Boukherroub, *Nanoscale Res. Lett.*, 2007, **2**, 577–596.
15 Y. Coffinier, S. Janel, A. Addad, R. Blossey, L. Gengembre, E. Payen and R. Boukherroub, *Langmuir*, 2007, **23**, 1608–1611.
16 N. Verplanck, E. Galopin, J.-C. Camart, V. Thomy, Y. Coffinier and R. Boukherroub, *Nano Lett.*, 2007, **7**, 813–817.
17 J. Zhang, X. Sheng and L. Jiang, *Langmuir*, 2009, **25**, 1371–1376.
18 F. Lapierre, V. Thomy, Y. Coffinier, R. Blossey and R. Boukherroub, *Langmuir*, 2009, **25**, 6551–6558.
19 M. Vallet, M. Vallade and B. Berge, *Eur. Phys. J. B*, 1999, **11**, 583–591.
20 F. Mugele and J.-C. Baret, *J. Phys.: Condens. Matter*, 2005, **17**, R705–R774.
21 S.-K. Fan, H. Yang, T.-T. Wang and W. Hsu, *Lab Chip*, 2007, **7**, 1330–1335.
22 G. Piret, Y. Coffinier, C. Roux, O. Melnyk and R. Boukherroub, *Langmuir*, 2008, **24**, 1670–1672.
23 G. Piret, H. Drobecq, Y. Coffinier, O. Melnyk and R. Boukherroub, *Langmuir*, 2010, **26**, 1354–1361.
24 Y. Koc, A. J. d. Mello, G. McHale, M. I. Newton, P. Roach and N. J. Shirtcliffe, *Lab Chip*, 2008, **8**, 582–586.
25 F. Li and F. Mugele, *Appl. Phys. Lett.*, 2008, **92**, 244108.
26 J. M. Oh, S. H. Ko and K. H. Kang, *Langmuir*, 2008, **24**, 8379–8386.
27 R. Malk, Y. Fouillet and L. Davoust, *Procedia Chem.*, 2009, **1**, 1107–1110.
28 J. Dixkens and H. Fissan, *Aerosol Sci. Technol.*, 1999, **30**, 438–453.
29 K. H. Yoo, J. S. Lee and M. D. Oh, *Aerosol Sci. Technol.*, 1997, **27**, 308–323.